Fluorescence spectroscopy of jet-cooled chiral (±)-indan-1-ol and its cluster with (±)-methyl- and ethyl-lactate

Katia Le Barbu-Debus,[a),b)] Francoise Lahmani, Anne Zehnacker-Rentien, and Nikhil Guchhait[a),c)]
Laboratoire de Photophysique Moléculaire du CNRS, Univ Paris-Sud, Orsay, F-91405, France

Sujit S. Panja and Tapas Chakraborty
Department of Chemistry, Indian Institute of Technology, Kanpur, Uttar Pradesh 208 016, India

(Received 12 July 2006; accepted 22 August 2006; published online 6 November 2006)

The laser-induced fluorescence excitation, dispersed fluorescence, and IR-UV double resonance spectra of chiral (±)-indan-1-ol have been measured in a supersonic expansion. Three low energy conformers of the molecule have been identified, and the ground state vibrational modes of each conformer are tentatively assigned with the aid of quantum chemistry calculations. The frequencies of the ν(OH) and ν(CH) stretch modes of the two most abundant conformers have been measured by fluorescence dip IR spectroscopy and have been used for their assignment. The dispersed fluorescence spectra clearly indicate the coupling of low-frequency modes, as was seen in other substituted indanes such as 1-aminoindan and 1-amino-2-indanol. (*R*)- and (*S*)-indan-1-ol distinctly form different types of clusters with (*R*)- and (*S*)- methyl- and ethyl-lactate. Both hetero- and homochiral clusters are characterized by complex spectra which exhibit a progression built on low-frequency intermolecular modes. © *2006 American Institute of Physics*.
[DOI: 10.1063/1.2355493]

I. INTRODUCTION

Conformational preferences and spectroscopic properties of pseudo-four-member rings such as indan and substituted indan have been investigated by several groups to get a detailed understanding of the potential energy surfaces associated with large amplitude motions. In particular, the value of the puckering barrier has been the object of a long standing controversy.[1–11] The double well potential for the puckering vibration of pseudo-four-member rings can be modified by several factors such as mode coupling, weak interactions (e.g., hydrogen bonding, van der Waals), incorporation of substituents, and steric effect.[12–16] Laane and co-workers[17,18] have demonstrated that taking into account the coupling between the ring flapping and puckering modes in indan results in a much lower puckering barrier than that obtained by a simple one dimensional double well potential as suggested by Hassan and Hollas.[19] Interestingly, it is found that substitution of the pseudo-four-member ring not only influences the low-frequency modes but also gives rise to several low energy conformers involving different positions (equatorial or axial) and orientations (anti or *gauche*) of the substituent with respect to the flexible carbon atom of the five member ring. Recently, Das *et al.* have identified three conformers of indan-2-ol by fluorescence spectroscopy in jet.[8] We have also investigated the spectroscopy of jet-cooled (±)-1-aminoindan and (±)-1-aminoindan-2-ol by laser-induced fluorescence and fluorescence dip IR spectroscopy. In both cases, two low energy conformers have been clearly identified and coupling between the low-frequency modes characteristic of the indan molecular frame has been evidenced.[10,11]

Since a single substitution at position 1 of the pseudo-four-member ring of indan generates a chiral center, the spectroscopic study of the complexation of the enantiomerically pure chromophore with chiral partners is also of special interest. Noncovalent weak interactions between chiral molecules are known to be responsible for controlling drug-receptor recognition and some enzyme catalytic reactions.[20–22] Laser spectroscopy combined with supersonic expansion techniques has been used successfully to get an in-depth understanding of the weak interactions at play in isolated chiral pairs without any other interference.[23–28] Since the method rests on the study of the modification of the spectroscopic properties of a chiral chromophore induced by complexation with chiral partners, it is of interest to explore the properties and efficiency of several aromatic selectands. Aromatic alcohols such as (±)-2-napththyl-1-ethanol, (±)-1-phenyl-1-ethanol, and (±)-1-phenyl-1-propanol have been the most studied chromophores until now.[24,26,29,30] Indan derivatives bearing an asymmetric carbon such as (±)-1-aminoindan and (±)-indan-1-ol have also been proposed as chiral discriminating agents for jet spectroscopy studies.[9,10] Scuderi *et al.* used one-color resonance-enhanced two photon ionization (1cR2PI) to get mass-resolved electronic spectra of jet-cooled chiral indan-1-ol and its complexes with water and some chiral solvents.[9] They have interpreted the spectrum of the bare molecule in terms of a single conformer. This observation contrasts with the other substituted indans which show several low energy conformers in jet. In the present work, therefore, laser-induced fluorescence exci-

[a)]Authors to whom correspondence should be addressed.
[b)]Electronic mail: katia.lebarbu@ppm.u-psud.fr
[c)]On leave from Department of Chemistry, University of Calcutta, 92 A.P.C. Road, Kolkata 700 009, India. Electronic mail: nguchhait@yahoo.com

tation, dispersed emission, and fluorescence dip IR spectroscopy are employed to re-investigate the electronic spectra of chiral (±)-indan-1-ol. *Ab initio* calculations have been performed to assist the analysis of the dispersed fluorescence and IR spectra and to assign the conformational isomers. In addition, the selectivity of (±)-indan-1-ol as a chiral discriminating agent has been tested by studying its complexes with chiral hosts such as (±)-methyl-and ethyl-lactate.

II. EXPERIMENT

The experiments have been performed on similar setups in France (Laboratoire de Photophysique Moléculaire, Orsay) and India (Indian Institute of Technology, Kanpur) for the measurement of laser-induced fluorescence (LIF) excitation spectra in a supersonic jet.[31] In brief, the sample vapor of indan-1-ol from Aldrich seeded in helium at a pressure of ~2 atm was expanded into vacuum through a continuous nozzle. The sample was heated to~40 °C to get enough vapor pressure. A tunable visible light is generated by pumping a dye laser (Sirah, Spectra Physik) by a Nd:YAG (yttrium aluminum garnet) (GCR 190, Spectra Physik) laser. The visible dye laser output is frequency doubled by a potassium dihydrogen phosphate (KDP) crystal and is used to excite isolated jet-cooled molecules. The fluorescence signal from the sample is collected perpendicular to both the exciting light and the molecular beam by a two lens collecting system and detected through a 25 cm monochromator working under broad band conditions with a Hamamatsu R2059 photomultiplier tube (PMT). The output of the PMT is averaged by an oscilloscope (Lecroy 9400) and finally processed by a personal computer. The dispersed emission setup is similar to the LIF setup except that a monochromator disperses the emission before detecting by a double-staged Peltier-cooled intensified charge-coupled device (ICCD) (Jobin Yvon, Model No. 3000V) detector camera.[32] A 0.75 m monochromator (Spex, model: 750M) with grating of groove density of 2400/mm was used for dispersion. Typical spectral resolution of the dispersion system is 7 cm^{-1}.

The IR-UV double resonance spectra have been measured in the ν(CH) and ν(OH) stretch mode regions. The measurement technique rests on the fluorescence dip detection method. A pulsed UV laser beam whose wavelength is fixed on an S_0-S_1 transition of a given species is slightly focalized on the cold region of the jet and the resulting fluorescence intensity is recorded as a measure of the ground state population. A tunable IR laser beam is introduced prior to the UV laser beam. When the IR beam is resonant with a vibrational level of the species, the IR absorption induces a decrease of the ground state population, which manifests itself by a reduction in fluorescence intensity. The experimental setup is described elsewhere.[33] The IR and UV beams are provided by two optical parametric oscillators (OPOs) synchronously pumped by a pulsed mode-locked Nd:YAG laser of 12 ps duration: Beta barium borate (BBO) crystal is used for the generation of visible (which is then frequency doubled) and $LiNbO_3$ for the IR light. The spectral width of the UV and IR lasers is 3 cm^{-1}.

The ground state structural calculations of the different low energy conformers of indan-1-ol have been performed either by density functional theory (DFT) calculations using B3LYP functional and 6-31G** basis set or MP2 level with 6-31G** basis set using the GAUSSIAN 98 software.[34] The ground state vibrational frequencies corresponding to the lowest energy structures were calculated at the B3LYP and MP2 levels and compared with the observed fluorescence emission spectra. The calculation of the potential energy surfaces (PESs) along the OH torsion has been performed in the following way: the OH group is rotated by ~10° intervals for each of the lowest energy axial and equatorial conformers and the remaining coordinates are fully re-optimized. Such calculation generates conformers with respect to the orientation of the OH group and allows us to estimate the barriers between them.

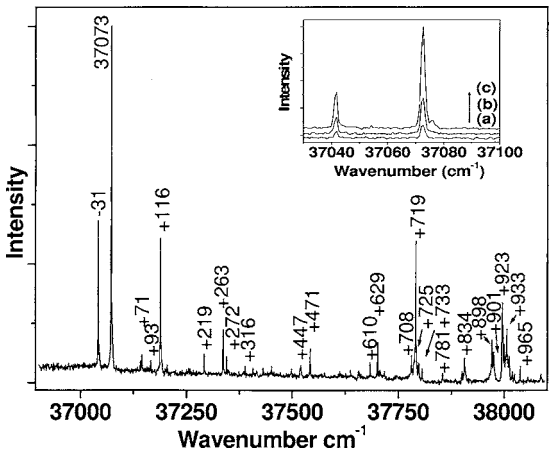

FIG. 1. Laser-induced fluorescence (LIF) excitation spectrum of jet-cooled indan-1-ol in the band origin region. Inset: Excitation spectra at three different sample temperatures: (a) 25 °C, (b) 40 °C, and (c) 60 °C.

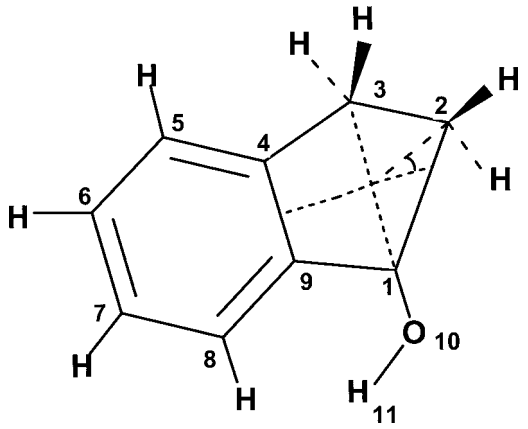

Structure of (±)-1-indan-1-ol with numbering of atoms.

III. RESULTS AND DISCUSSION

A. Bare molecule

1. LIF spectrum

The laser-induced fluorescence excitation spectrum of indan-1-ol in the $S_0 \rightarrow S_1$ transition origin region is shown in Fig. 1. It shows an intense band at 37 073 cm^{-1} followed by weaker bands at the higher energy side. The 37 073 cm^{-1}

intense band is accompanied by a moderately intense band at 31 cm^{-1} lower in energy. The 37 073 and 37 042 cm^{-1} bands will be called bands A and B hereafter, respectively. Two other bands that display noticeable intensity appear at +116 and +719 cm^{-1}. In addition, very weak features appear at +71, 263, 272, 447, 471, 629, 708, 834, 898, 901, 923, and 933 cm^{-1}. It is worth noting that the −31 and +71 cm^{-1} bands are not present in the mass-resolved excitation spectrum. All the other bands in the LIF spectrum are similar to those of the mass-resolved 1cR2PI spectrum observed by Scuderi *et al.*[9] However, as the fluorescence quantum yield and ionization efficiency may vary along the spectrum, the relative intensity distribution of the blue-side bands in the LIF spectrum is found to be different from that of the 1cR2PI spectrum. The absence of the −31 and +71 cm^{-1} bands in the mass-resolved excitation spectrum could be due to the fact that they arise from higher mass clusters. If they do, their relative intensity with respect to the strongest 0-0 band must increase by increasing the sample temperature, hence the vapor pressure. As seen in Fig. 1 (inset), the change in sample vapor pressure does not modify the intensity ratio of the bands at 37 042 (−31) and 37 073 cm^{-1}. This result indicates that the band at −31 cm^{-1} does not arise from a dimer or higher cluster of indan-1-ol. Secondly, hot band transitions can be responsible for the red shifted (−31 cm^{-1}) band. This can be verified by changing the cooling conditions. However, changing the backing pressure does not change the intensity ratio of the two bands in the LIF excitation spectrum. Moreover, we obtained exactly the same spectrum when using a continuous or pulsed supersonic expansion. This result clearly supports the fact that the −31 cm^{-1} band is not a hot band. It should thus be assigned to a different conformational isomer. The reason for its absence in the mass-resolved 1cR2PI spectrum is not clear at the moment and will be discussed later.

2. Emission spectra

The emission spectra following single vibronic level (SVL) excitation of the bands at 37 073 (band A), 37 042 (band B), and 37 144 cm^{-1} (band C) are shown in Fig. 2. The frequencies of the main vibronic bands are presented in Table I. The signatures of the SVL spectra seem to show that these three bands are the origin of emission from three different species. The emission obtained by pumping the strongest band in the LIF spectrum [Fig. 2(a)] is dominated by the low-frequency mode at 147 cm^{-1} which appears as a three member progression and in combination with the most prominent benzene ring modes found at 741, 1022, 1209, and 1482 cm^{-1}. Other low-frequency vibrations are seen at 259 and 275 cm^{-1}. This spectrum is very similar to the emission spectra resulting from excitation of the origin transition of the parent molecule indan and 1-aminoindan. Thus the nature of the substituent in position 1 does not strongly affect the vibrational pattern appearing in the spectroscopy of indan derivatives.

The emission spectrum resulting from the excitation of the −31 cm^{-1} band [Fig. 2(b)] is quite different from the emission of band A, particularly in the low-frequency region. It exhibits main bands at 112 and 307 cm^{-1} and a weaker

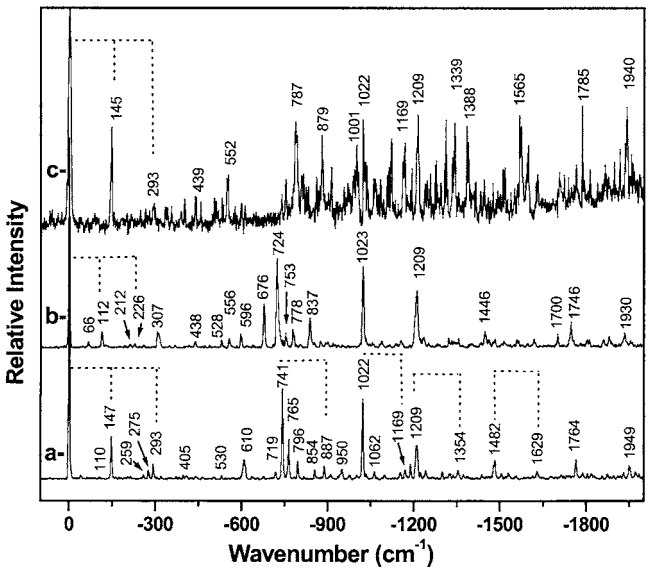

FIG. 2. Single vibronic level emission spectra of indan-l-ol excited at (a) 37 073 cm^{-1} (band A), (b) 37 042 cm^{-1} (band B), and (c) 37 144 cm^{-1} (band C).

feature at 66 cm^{-1}. Also the 700 cm^{-1} region differs from what was observed in the case of band A. Higher frequency bands at 1023 and 1209 cm^{-1} are not modified relative to band A. The emission obtained after excitation of the weak +71 cm^{-1} band [Fig. 2(c)] excitation resembles that of band A in the low-frequency region and shows the same low-frequency progression built on a 145 cm^{-1} mode. However, it is much more congested in the high-frequency benzene ring mode region.

The emission spectrum resulting from the excitation of the +116 cm^{-1} band [Fig. 3(a)] shows a 0-0-type emission similar to that observed from the origin (band A) starting on the $\Delta v=0$ transition at 147 cm^{-1} from excitation. It can thus be deduced from this spectrum that the excited 116 cm^{-1} vibration in S_1 corresponds to the S_0 147 cm^{-1} mode. A band of noticeable intensity appears in the region of the $\Delta v=0$ transition, at 110 cm^{-1} from the excitation. In addition, weak bands appear at 205, 259, and 275 cm^{-1} from the excitation line. This indicates that several low-frequency modes are coupled and hence, the excited vibronic level at +116 cm^{-1} can be described as a combination of low-frequency vibrations which give rise in emission to transitions toward different ground state vibrational levels according to Duchinsky effect.[35–37] The low-frequency ground state mode at 110 cm^{-1} may be the counterpart of the 93 cm^{-1} vibration seen as a weak band in the LIF spectrum. The emission from higher vibronic levels at 219, 263, and 719 cm^{-1} bands [Figs. 3(b)–3(d)] clearly shows their corresponding ground state vibrations at 259, 275, and 741 cm^{-1}, respectively. Besides, for excitation of each vibronic level, it is observed that the $\Delta v=0$ transition region exhibits a multiplet structure, which also clearly indicates the existence of mode coupling. Last, a broadening of the emission spectrum obtained by pumping the 719 cm^{-1} level is observed and is the manifestation of intramolecular vibrational redistribution. Each of these spec-

TABLE I. Main ground state vibrational modes of indan-1-ol obtained from SVL spectra and calculated harmonic frequencies at DFT level (B3LYP/6-31G**). The values in parentheses in the calculated frequencies are at the MP2/6-31G** level. ν_1=puckering coupled with Bz-ring twist, ν_2=flapping coupled with puckering, ν_3=Bz-ring ν_6 coupled with C_5 ring deformation, ν_4=Bz-ring ν_6 coupled with C_5 ring deformation, ν_5=Bz-ring ν_{18}, ν_6=Bz-ring in plane CH bend, and ν_7=OH stretch (Bz-ring ν_6 and Bz-ring ν_{18} are benzene vibrations in Wilson's notation).

Conf. I_{eq}		Conf. II_{ax}		Conf. II_{eq}	
Experimental frequency	Calculated frequency and assignment	Experimental frequency	Calculated frequency and assignment	Experimental frequency	Calculated frequency and assignment
110	113 (119) ν_1	66	88 (106) ν_1		103 (120) ν_1
147	151 (153) ν_2	112	122 (130) ν_2	145	140 (155) ν_2
205	211 (213) ring twisting coupled with substituent torsion	⋯	⋯	⋯	⋯
275	(263) ring deformation			⋯	
293	2×147			293	2×145
⋯	⋯	307	307 (310) OH torsion coupled to puckering	⋯	⋯
610	615 (615) ν_3	596	604 (619) ν_3	⋯	612 (620) ν_3
741	781 (781) ν_4	724	789 (786) ν_4	787	774 (781) ν_4
1022	1051 (1059) ν_5	1023	1048 (1064) ν_5	1022	1045 (1045) ν_5
1209	1236 (1234) ν_6	1209	1232 (1257) ν_6	1209	1218 (1230) ν_6
3638	3789 (3856) ν_7	3610	3797 (3862) ν_7		

tra shows the dominant benzene ring modes (1022 and 1209 cm^{-1}), as was seen in the emission from the 37 073 cm^{-1} band (band A).

3. IR spectra

The IR spectra obtained by setting the pump laser on the transitions located at 37 073 cm^{-1} (band A) and 37 042 cm^{-1} (band B) are shown in Fig. 4. The band located at 37 144 cm^{-1} was too weak to be probed. Both spectra display a single band in the region of 3600 cm^{-1}, which can be readily assigned to the ν(OH) stretch mode. It appears at 3610 and 3638 cm^{-1} for bands A and B, respectively. The lowest energy part of the spectrum contains the ν(CH) stretch transitions. The aromatic CH stretch frequencies appear around 3400 cm^{-1} as a weak and unresolved feature for both isomers. The aliphatic ν(CH) stretch transitions appear as five strong bands below 3000 cm^{-1} at slightly different frequencies for the two isomers. They show up at 2876, 2916, 2936, 2963, and 2984 cm^{-1} for band A and at 2872, 2916, 2946, 2964, and 2989 cm^{-1} for band B.

4. Calculations

The structural calculations of indan-1-ol at the density functional theory (DFT) level with B3LYP functional and 6-31G** basis set and at MP2 level with 6-31G** basis set generate several low energy conformers in the ground state. The hydroxyl group can be in axial or equatorial position and for each of the axial or equatorial configurations the OH group can have three different orientations in space (defined by the dihedral angle θ=$C_{aroma}-C_1-O-H$), as it was seen in the case of 1-aminoindan. Repulsion between the lone pair of the hydroxyl oxygen and the benzene π electrons destabilizes some of the conformers and weak π-hydrogen bonding interaction stabilizes others. The most stable calculated structures are shown in Fig. 5 and their relative energies predicted

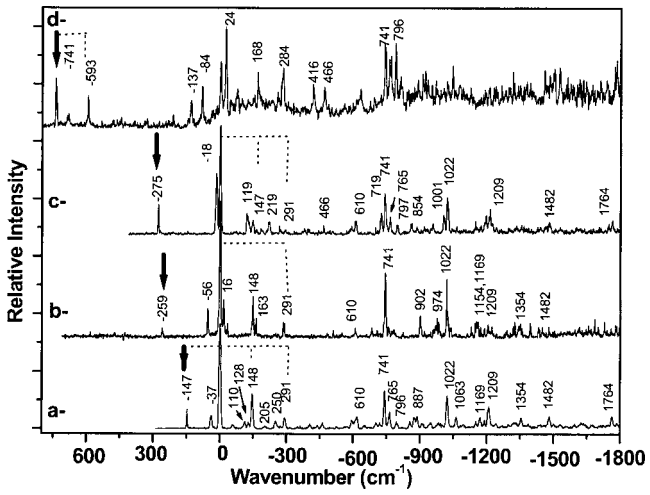

FIG. 3. Single vibronic level emission spectra of indan-l-ol excited at (a) 37 073+116 cm^{-1}, (b) 37 073+219 cm^{-1}, (c) 37 073+263 cm^{-1}, and (d) 37 073+719 cm^{-1} bands. The zero of the scale is set on the 37 073 cm^{-1} transition. The arrow shows the excitation wavelength.

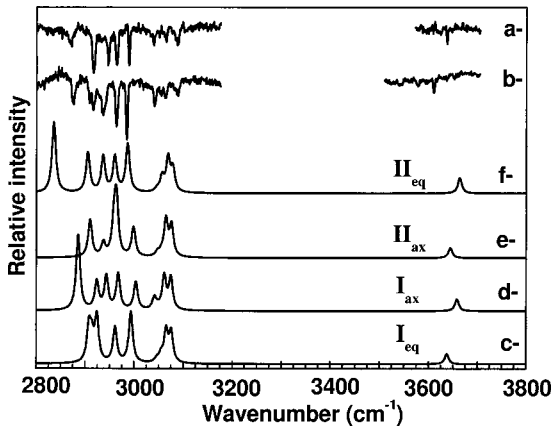

FIG. 4. IR-UV fluorescence dip spectra of indan-l-ol when UV light is fixed at (a) 37 042 cm^{-1} (band B) and (b) 37 073 cm^{-1} (band A). Simulated spectra at MP2 level of (c) conformer I_{eq}, (d) conformer I_{ax}, (e) conformer II_{ax}, and (f) conformer II_{eq}. A 0.94 scaling factor has been applied to the MP2 frequencies for an easier comparison with the experimental values.

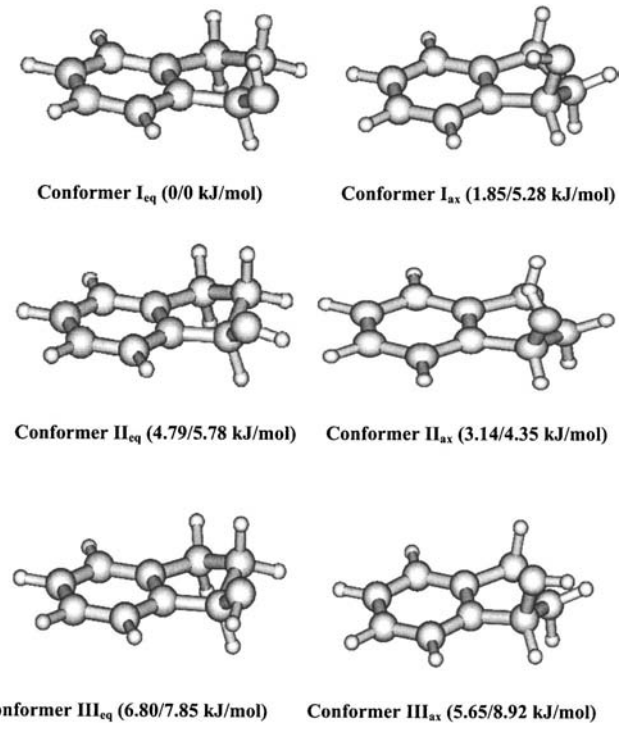

FIG. 5. Calculated low-energy conformers of indan-l-ol for the ground state at the MP2 level with 6-31G** basis set. The numbers in parentheses are the relative energies (first value from MP2 and second value from DFT calculations) with respect to the minimum energy structure.

at the MP2 and DFT/B3LYP levels of theory are presented in Table II. The three most stable structures (conformer I_{eq}, conformer I_{ax}, and conformer II_{ax}) have the hydrogen of hydroxyl group directed towards the benzene π electrons, while in the three comparatively higher energy conformers the OH group is directed outwards the benzene ring. Both MP2 and B3LYP calculations generate the same lowest energy structure I_{eq} which is similar to the lowest energy structure of 1-aminoindan, both having the substituent in equatorial position. In the second stable conformer of indan-1-ol the OH group is, however, in the axial position, which differs from the second stable conformer of 1-aminoindan where the NH_2 group was still in equatorial position.[10] In this case, however, the second conformer in MP2 calculations (structure I_{ax} in Fig. 5) differs from that obtained with B3LYP calculations (structure II_{ax} in Fig. 5) by the OH torsion angle θ. The possible path for conversion from one equatorial to another equatorial conformer or from one axial to another axial conformer is possible by rotation of the OH group. Such potential energy curves obtained along the OH torsion coordinate are presented in Fig. 6 for the equatorial and axial conformers. Unlike indan-2-ol, the *gauche* conformers of indan-1-ol are not equivalent since the interactions of lone pairs and hydrogen with benzene π electrons are not the same. However, the two *gauche* axial structures are calculated very close in energy [$\Delta E(I_{ax}/II_{ax})=-1.29$ kJ/mol in MP2 and +0.93 kJ/mol in B3LYP calculations] and the barrier height between the two forms is only about 3 kJ/mol. In these conditions it is difficult to decide which form is the observed isomer without new spectroscopic arguments. In contrast, the energy difference between the two lowest energy equatorial conformers (I_{eq} and II_{eq}) is large and the barrier height for conversion from one conformer to the other is also high (barrier ~12 kJ/mol for I_{eq} to II_{eq} and ~7.2 kJ/mol for II_{eq} and I_{eq}). Therefore, transformation from one equatorial conformer to another by OH torsion is unexpected.

TABLE II. Relative energy of the most stable calculated ground state conformers at different levels of theory.

	Energy (kJ/mol)	
Conformers	MP2/6-31G**	DFT/B3LYP/6-31G**
Conformer I_{eq}	0	0
Conformer II_{eq}	4.79	5.78
Conformer III_{eq}	6.80	7.85
Conformer I_{ax}	1.85	5.28
Conformer II_{ax}	3.14	4.35
Conformer III_{ax}	5.65	8.92

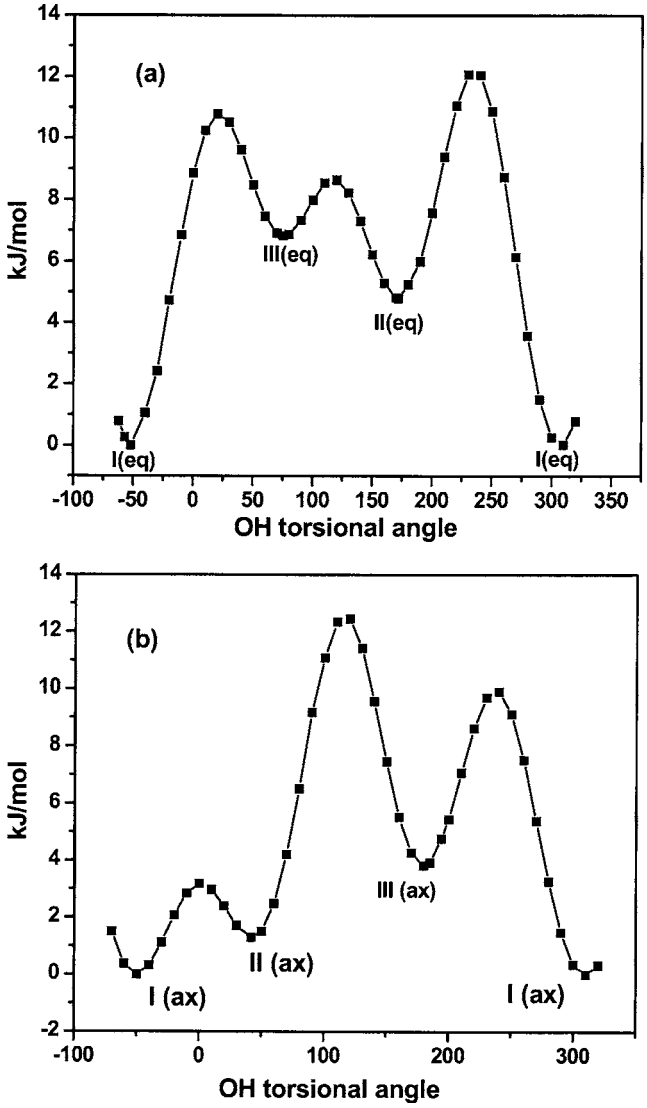

FIG. 6. Potential energy curves obtained by MP2/6-31G** calculations for the torsional motion of OH group: (a) equatorial and (b) axial. The zero of the scale is set on the minimum energy structure.

To correlate the first three bands observed in the fluorescence excitation spectrum to the predicted structures, we first

compare the relative stability of the conformers with the relative intensity of the bands. Accordingly we attribute the strongest band at 37 073 cm^{-1} in the LIF spectrum to the energetically most stable conformer I_{eq}. The −31 and +71 cm^{-1} bands should correspond to either conformers I_{ax}, II_{ax}, on II_{eq}. As discussed before, the energy barrier between conformers I_{ax} and II_{ax} is too low for both isomers to be trapped in the supersonic jet and only one of them is expected to be present.[38] Thus the −31 cm^{-1} band should correspond to either axial I_{ax} or II_{ax} isomers and the small +71 cm^{-1} feature should be attributed to the II_{eq} isomer with the OH group directed outwards the molecular frame. As mentioned before, the energy barrier (Fig. 6) between I_{eq} and II_{eq} conformers is high enough for both isomers to be trapped in their corresponding well during the course of the supersonic expansion. Being a theoretically high-energy conformer, conformer II_{eq} should be less populated and should correspond to a weaker band in the LIF spectrum.

We can now compare the observed and DFT calculated frequencies in the high-frequency region. The spectrum obtained by setting the probe on band A shows a lower ν(OH) stretch frequency than that obtained with the probe on band B. Conformer I_{eq} has the lowest calculated ν(OH) stretch mode frequency (3788 cm^{-1}) of the four most stable conformers. This gives further support to the assignment of band A to I_{eq}.

The spectrum obtained by setting the probe on band B resembles that of one of the axial conformers I_{ax} or II_{ax}, and a definite assignment of band B to one of them is difficult on the basis of the IR spectrum only. As mentioned before, the calculated barrier between I_{ax} and II_{ax} is very low and all that one can conclude from the IR spectra is that conformer II involves a hydroxyl substituent in axial position.

One can find also an additional argument for the assignment of the conformers by comparing the ground state vibrational frequencies deduced from the emission spectra with the theoretical normal modes deduced from B3LYP/6-31G** calculation (Table I). For conformer I_{eq}, there is a very good agreement between the low-frequency bands observed at 110, 147, and 205 cm^{-1} and the calculated harmonic vibrational frequencies of 113, 151, and 211 cm^{-1}. These frequencies are similar to those of 1-aminoindan assigned to puckering coupled with ring twisting, ring puckering coupled with interring flapping, and ring twisting coupled with substituent torsion, respectively. This shows that the chemical nature of the substituent does not strongly influence the high amplitude deformations of the indan skeleton for this conformer. Similarly the most intense emission features observed at 741 and 1022 cm^{-1} correlate very well with the modes calculated at 781 and 1051 cm^{-1} and assigned to five member ring deformations and aromatic ring deformation.

The agreement between the calculated spectrum of I_{ax} or II_{ax} with experimental frequencies observed in the emission spectra resulting from the excitation of band B is not as satisfactory as in the previous conformer. However, the general trends such as the decrease of the frequency of the mixed puckering modes (ν_{exp}=66 cm^{-1}), and the presence of an additive vibrational frequency at 307 cm^{-1} in this conformer with respect to the most stable one, are well reproduced by the calculations. The discrepancy may be related to the small energy barrier between conformers I_{ax} and II_{ax}, which amounts to about 3 kJ/mol. In this situation, the harmonic frequencies approximation might not hold.

Finally the emission resulting from the excitation of the weak band at 71 cm^{-1} resembles that of the main conformer. This resemblance matches the similitude which has been observed between the calculated frequencies of I_{eq} and II_{eq}. We therefore assign this band to the II_{eq} structure.

Still, the difference between the 1cR2PI spectrum obtained by Scuderi *et al.* and the LIF spectrum reported here is not clearly understood. Discrepancies between S_0-S_1 spectra obtained by 1cR2PI and those obtained by LIF have been observed already in systems showing a puckering inversion such as coumaran.[16] In this case, the zero electron kinetic energy (ZEKE) results suggested the presence of two isomers but were at odds with the backing pressure dependence of the relative intensity of the two bands. The authors eventually assigned the band of minor intensity to a hot band. In our system, it would be difficult to explain the difference between the IR spectra of bands A and B if band B were a hot band. The difference would then arise from anharmonic coupling between the IR excited mode and the vibration involved in the hot band, which is probably located on the pseudo-four-member ring, as supposed for coumaran. However, it is not likely that anharmonic coupling with a low-frequency mode located on the pseudo-four-member ring amounts to 28 cm^{-1} for the OH stretch mode. We therefore favor the assignment of this band to the I_{ax} conformer. The reason why this conformer is not observed in the 1cR2PI spectrum could be that it undergoes fast fragmentation in the ion.[26,28] Indeed, benzyl alcohol derivatives undergo fast fragmentation. It is suggested that two-color resonance enhanced multiphoton ionization (2c-REMPI) experiments would be highly desirable to answer this question.

B. Clusters

Figure 7 shows the excitation spectra of indan-1-ol in the presence of methyl-lactate and ethyl-lactate. As can be seen in this figure, the spectrum of the heterochiral mixture (*R*/*S* or *S*/*R*) displays a pattern, which differs from that of the homochiral mixture (*R*/*R* or *S*/*S*). Thus complexation with indan-1-ol allows discriminating spectrally between the enantiomers of methyl- and ethyl-lactate. The spectrum of the complexes formed between (*R*)-indan-1-ol and (*S*)-methyl-lactate displays numerous bands mainly located at the red side of the strongest band (37 073 cm^{-1}). Much fewer and weaker bands appear at the blue side. The lowest energy band is shifted down in energy by 207 cm^{-1} relative to the 37 073 cm^{-1} monomer band. It acts as an origin for a vibrational progression built on a 15 cm^{-1} mode and is followed by a complex pattern. In the blue side of the main origin transition, very weak bands appear at +44 and

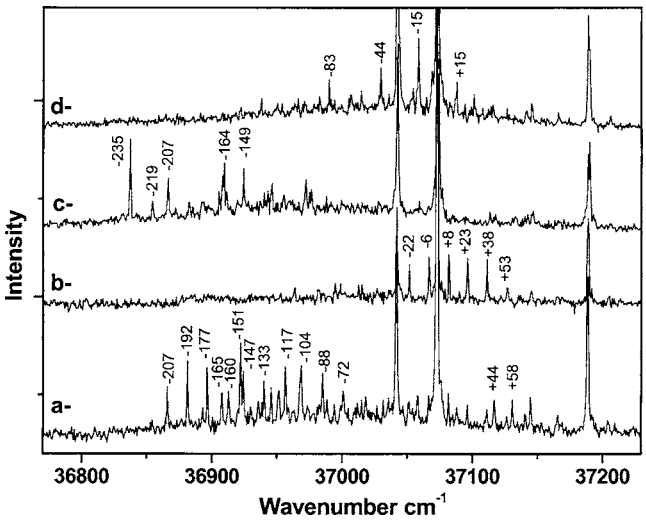

FIG. 7. Laser-induced fluorescence (LIF) excitation spectrum of jet-cooled (*R*)-indan-l-ol with (a) (*S*)-methyl-lactate and (b) (*R*)-methyl-lactate and (*R*)-indan-l-ol with (c) (*S*)-ethyl-lactate and (d) (*R*)-ethyl-lactate.

+58 cm^{-1}. This suggests the presence of isomers or clusters of different sizes. Contrasting with this complexity, the excitation spectrum of (*S*)-indan-1-ol with (*S*)-methyl-lactate exhibits a very simple spectrum, starting at −22 cm^{-1} from the main origin band, which consists of a single vibrational progression built on a 15 cm^{-1} progression. Spectra obtained for complexes of (*R*)-indan-1-ol with (*S*)-ethyl-lactate exhibit a similar trend: The spectrum of the homochiral mixture bears strong similarities to that of the methyl-lactate complex, with a 15 cm^{-1} progression hardly shifted relative to the bare molecule origin. The spectrum of the heterochiral pair exhibits a larger redshift than that of the homochiral one. Stronger redshifts together with long intermolecular progressions have been attributed in other chiral systems to folded geometries showing large dispersion energy.[39] A similar effect could also be observed in this system. Other possibilities include selective complexation of the two enantiomers by different isomers of the chromophore or enantioselectivity in the size of the formed adducts. Further experiments are in progress to answer these questions.

IV. CONCLUSION

In this paper, we have measured LIF excitation, SVL emission, and fluorescence dip IR spectra of indan-1-ol and identified three conformers in supersonic jet. In combination with MP2 and DFT calculations, we have calculated ground state structures and the vibrational modes of the lowest conformer to assign the experimental spectra. The signature of mode coupling among the low-frequency modes is observed, as was seen in the case of other substituted indans. It is found that indan-1-ol shows enantioselective complexation with methyl- or ethyl-lactate.

ACKNOWLEDGMENTS

One of the authors (N.G.) gratefully acknowledges CNRS for providing visiting scientist position to work at Laboratoire de Photophysique Moléculaire, University of Paris XI, Orsay and would like to thank his research scholar Amrita Chakraborty for helping the preparation of the paper. The authors acknowledge the "Centre de Ressources Informatiques" (Orsay University) for the allotment of computer resources. Another author (T.C.) thanks the Department of Atomic Energy Commission for the financial support to measure the DF spectra.

[1] J. M. Hollas and E. Khailipour, J. Mol. Spectrosc. **77**, 124 (1979).
[2] T. L. Smithson, J. A. Duckett, and H. Weiser, J. Phys. Chem. **88**, 1102 (1984).
[3] K. H. Hassan and J. M. Hollas, Chem. Phys. Lett. **169**, 179 (1990).
[4] K. H. Hassan and J. M. Hollas, Chem. Phys. Lett. **157**, 183 (1989).
[5] J. Zhang, W. Y. Chiang, and J. Laane, J. Chem. Phys. **100**, 3455 (1994).
[6] T. Klots, S. N. Lee, and J. Laane, J. Phys. Chem. **103**, 833 (1999).
[7] M. J. Watkins, D. E. Belcher, and M. C. R. Cockett, J. Chem. Phys. **116**, 7855 (2002).
[8] A. Das, K. K. Mahato, S. S. Panja, and T. Chakraborty, J. Chem. Phys. **119**, 2523 (2003).
[9] D. Scuderi, A. Paladini, M. Satta, D. Catone, S. Piccirillo, M. Speranza, and A. Giardini-Guidoni, Phys. Chem. Chem. Phys. **4**, 4999 (2002).
[10] K. Le Barbu-Debus, F. Lahmani, A. Zehnacker-Rentien, and N. Guchhait, Phys. Chem. Chem. Phys. **8**, 1001 (2006).
[11] K. Le Barbu-Debus, F. Lahmani, A. Zehnacker-Rentien, and N. Guchhait, Chem. Phys. Lett. **422**, 218 (2006).
[12] G. R. Desiraju and T. Steiner, *The Weak Hydrogen Bond in Structural Chemistry and Biology* (Oxford University Press, Oxford, 1999).
[13] T. M. Fong, M. A. Cascieri, H. Yu, A. Bansal, C. Swain, and C. D. Strader, Nature (London) **363**, 350 (1993).
[14] J. Laane, J. Phys. Chem. A **104**, 7715 (2000).
[15] J. Laane, in *Structures and Conformations of Non-rigid Molecules*, edited by J. Laane, M. Dakkouri, B. van der Veken, and H. Oberhammer (Elsevier, Amsterdam, 1993), Chap. 4.
[16] M. J. Watkins, D. E. Belcher, and M. C. R. Cockett, J. Chem. Phys. **116**, 7868 (2002).
[17] E. Bondoc, T. Klots, and J. Laane, J. Phys. Chem. A **104**, 275 (2000).
[18] Z. Arp, N. Meinander, J. Choo, and J. Laane, J. Chem. Phys. **116**, 6648 (2002).
[19] K. H. Hassan and J. M. Hollas, J. Mol. Spectrosc. **147**, 100 (1991).
[20] M. Amat, O. Bassas, M. A. Pericas, M. Pasto, and J. Bosch, Chem. Commun. (Cambridge) **2005**, 1327.
[21] K. Kinbara, Y. Kobayashi, and K. Saigo, J. Chem. Soc., Perkin Trans. 2 **2000**, 111.
[22] M. Masui and T. Shioii, Tetrahedron Lett. **39**, 5195 (1998).
[23] D. Consalvo, A. Van der Avoird, S. Piccirillo, M. Coreno, A. Giardini-Guidoni, A. Mele, and M. Snels, J. Chem. Phys. **99**, 8398 (1993).
[24] K. Le Barbu-Debus, N. Seurre, F. Lahmani, and A. Zehnacker-Rentien, Phys. Chem. Chem. Phys. **4**, 4866 (2004).
[25] N. Borho, T. Haber, and M. A. Suhm, Phys. Chem. Chem. Phys. **3**, 1945 (2001).
[26] M. Mons, F. Piuzzi, I. Dimicoli, A. Zehnacker-Rentier, and F. Lahmani, Phys. Chem. Chem. Phys. **2**, 5065 (2000); K. Le Barbu-Debus, A. Zehnacker-Rentien, F. Lahmani, M. Mons, F. Piuzzi, and I. Dimicoli, Chirality **13**, 715 (2001).
[27] D. Catone, A. Giardini-Guidoni, A. Paladini, S. Piccirillo, F. Rondino, M. Satta, D. Scuderi, and M. Speranza, Angew. Chem. **43**, 1868 (2004).
[28] A. Latini, D. Toja, A. Giardini-Guidoni, S. Piccirillo, and M. Speranza, Angew. Chem., Int. Ed. **38**, 815 (1999).
[29] F. Lahmani, K. Le Barbu-Debus, and A. Zehnacker-Rentien, J. Phys. Chem. A **103**, 1991 (1999).
[30] D. Scuderi, A. Paladini, M. Satta, D. Catone, F. Rondino, M. Tacconi, A. Filippi, S. Piccirillo, M. Speranza, and A. Giardini-Guidoni, Phys. Chem. Chem. Phys. **5**, 4370 (2003).
[31] K. Le Barbu-Debus, F. Lahmani, and A. Zehnacker-Rentien, J. Phys. Chem. A **106**, 6271 (2002).
[32] C. K. Nandi, M. K. Hazra, and T. Chakraborty, J. Chem. Phys. **123**, 124310 (2005).
[33] N. Seurre, K. Le Barbu-Debus, F. Lahmani, A. Zehnacker-Rentien, and J. Sepiol, Chem. Phys. **295**, 21 (2003).
[34] M. J. Frisch, G. W. Trucks, H. B. Schlegel *et al.*, GAUSSIAN 98, Revision A. 9, Gaussian, Inc., Pittsburgh, PA, 1998.

[35] G. J. Small, J. Chem. Phys. **54**, 3300 (1971).
[36] W. L. Smith, J. Mol. Spectrosc. **187**, 6 (1998).
[37] G. M. Sando, K. G. Spears, and J. T. Hupp, J. Phys. Chem. A **105**, 5317 (2001).
[38] R. S. Ruoff, T. D. Klots, T. Emilson, and H. S. Gutowsky, J. Chem. Phys. **93**, 3124 (1990).
[39] K. Le Barbu-Debus, V. Brenner, Ph. Millié, F. Lahmani, and A. Zehnacker-Rentien, J. Phys. Chem. A **102**, 128 (1998).